XLVI CILAMCE
VITÓRIA - ES - BRAZIL - 2025
XLVI IBERO-LATIN AMERICAN CONGRESS ON COMPUTATIONAL METHODS IN ENGINEERING

Torsional vibration analysis of geared turbomachinery trains using the finite element method

João Carlos F. Milagres[1], Marco Túlio C. Faria[2]

[1]*Graduate Program in Mechanical Engineering, Universidade Federal de Minas Gerais*
Pampulha Campus - Av. Antônio Carlos 6627, 31270-901, Minas Gerais, Brazil
joaoc_fm@hotmail.com
[2]*Department of Mechanical Engineering, Universidade Federal de Minas Gerais*
Pampulha Campus - Av. Antônio Carlos 6627, 31270-901, Minas Gerais, Brazil
mtfaria.ufmg@gmail.com

Abstract. In the Oil & Gas industry, the replacement of gas turbines by electric motors as drivers of large rotating equipment is a growing tendency. When the process equipment is a turbomachinery, the use of Variable Frequency Drive (VFD) motors enable effective and efficient operation over a wide speed range. VFDs also generate torsional excitations, that if not properly addressed in the design phase, can lead to catastrophic failures of critical equipment. This work presents the application of the finite element method on the torsional analysis of geared turbomachinery trains based on the guidelines of the API (American Petroleum Institute). The procedure is applied for a fixed-speed electric motor driven compressor and its modified variable-speed version by the inclusion of a VFD. The system torsional natural frequencies (TNFs), mode shapes, Campbell Diagrams, steady-state alternating shear stresses and transient response caused by 2-phase and 3-phase motor short-circuits are predicted in the analysis. The results are used for the mechanical integrity assessment of the turbomachinery train.

Keywords: torsional vibration; geared turbomachinery trains; VFD torsional excitation; finite element method

1 Introduction

In different industries, there is a growing tendency towards the application of more efficient process control methods aiming to save energy and reduce greenhouse gas emissions. In the offshore Oil & Gas (O&G) industry, plant electrification has been recommended as one strategy for companies to reduce their Greenhouse Gases emissions, which can be achieved by replacing the gas turbines that drive large rotating equipment by electric motors, that can be fed by the grid supplied with renewable sources (e.g., power from shore) or by a more efficient centralized offshore power generation facility, IOGP [1]. When the process equipment is a turbomachinery such as a compressor and the driver is a motor, the use of Variable Frequency Drive (VFD) motors enables effective and efficient operation over a wide speed range, which is not the case when the machine is driven by a constant speed motor, since their capacity is controlled by recycling, or variable inlet guide vanes or throttling, which are effective but inefficient. Therefore, VFD motors have gained relevance as drivers for large turbomachinery recently, Corcoran [2] and Kita [3]. A typical geared motor driven compressor train scheme is shown in fig. 1.

The use of VFDs in turbomachinery trains can also pose a threat to the mechanical integrity of the train. Since the VFDs use AC-DC-AC conversions of the supplied voltage and current electric waves, the resulting VFD output is not perfectly sinusoidal, but contains harmonic distortion, which leads to air-gap torque pulsation, with multiple harmonics of the VFD output frequency and inter-harmonics (functions of the difference between line frequency and VFD output frequency) being generated, causing torsional vibration along the train rotors and making it virtually impossible to completely eliminate torsional resonance, which occurs when an excitation frequency is coincident with any train torsional natural frequency (TNF) within operational range, Kita [3].

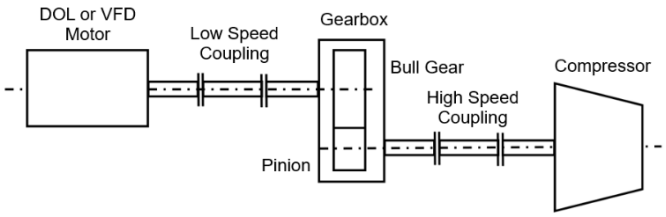


Figure 1. Typical geared motor driven compressor train scheme

Torsional vibration can be defined as the oscillatory twisting of the shafts that is superimposed to the running speed, being evidenced as an oscillatory variation of the speed. In general, TNFs of individual rotors are above the range of torsional excitations, but when the rotors are connected by couplings (relatively low torsional stiffness) and gears, system TNFs are reduced, Vance [4]. Besides, multibody and geared trains have increased likelihood of suffering torsional problems due to the increased number of TNFs, Corcoran [2]. Another important characteristic of torsional vibration is the small damping level, often negligible and limited to the material internal friction. For a typical O&G train compressor, 0.6-1.7% of critical damping is frequently assumed, Corcoran [2].

Torsional measurement devices are not typically installed in turbomachinery and the mechanical factory accepting test (FAT) does not cover entire train testing due to the costs and project schedule impact, Corcoran [2]. During operation, torsional vibration seldom produces noise or transmit vibration to the base and frequently, the first sign of a torsional problem is a broken coupling, shaft or gear tooth, Vance [4]. Many authors, such as Corcoran [2] and Kita [3], report cases of failures caused by torsional vibration, most of them VFD-related.

Torsional behavior prediction of turbomachinery trains in the design phase is essential to ensure train integrity, especially in the O&G industry, where lost production costs might be enormous. To this end, American Petroleum Institute (API) provides in its Rotordynamic Tutorial (API [5]) guidelines regarding modeling and analysis of torsional vibration in turbomachinery trains, which is even more critical in VFD driven trains. This work presents the application of finite element method to the torsional analysis of geared turbomachinery trains based on API guidelines. The code is applied to a case study of a fixed-speed and VFD driven compressor train.

2 Mathematical modeling using the Finite Element Method (FEM)

A single-speed turbomachinery train under torsion can be represented as a finite element model which contains N nodes and N-1 torsional shaft elements connecting the nodes, as shown in fig. 2. Each node has one degree of freedom (DOF), represented by an angular displacement $\theta_i(t)$. For the model with N nodes (DOFs), N second-order differential equations result. All rotary inertia such as impellers, gears, couplings, etc. are lumped into discrete disks located at the nodes (J_i), containing inertia but no flexibility, while the shaft elements contain flexibility and inertia (El_i). Dissipation of energy is represented by dampers connecting a node to the "ground" (C_i) if the damper causes an absolute velocity-dependent torque (e.g., bearings) or two nodes (relative twisting motion). Torque loads can be applied to any node. The equations of motion of the system subjected to forced vibration can be described by eq. 1, which can be obtained by the application of Lagrange method, Inman [6]:

$$[J]\{\ddot{\theta}\} + [C]\{\dot{\theta}\} + [K]\{\theta\} = \{T(t)\} \tag{1}$$

where $[J]$, $[C]$ and $[K]$ are the polar mass moment of inertia, damping and torsional stiffness matrices; $\{\ddot{\theta}\}$, $\{\dot{\theta}\}$ and $\{\theta\}$ are the angular acceleration, velocity and displacement vectors; $\{T(t)\}$ is the excitation torques vector.

For geared turbomachinery trains, the determination of global inertia, stiffness and damping matrix can be conveniently obtained by the application of the FEM to an equivalent single speed model, accounting for the differences in kinetic and strain energies associated with different speeds, that is capable to describe the equations of motion for each element separately and then combine all by the superposition principle of the direct stiffness method, Walker [7]. The components of the element matrices are added to the global matrices in the row and column that correspond to the two global end nodes of each element. Additionally, lumped inertias are added to the main diagonal of the inertia matrix at the node locations where they act (same for "ground" dampers).

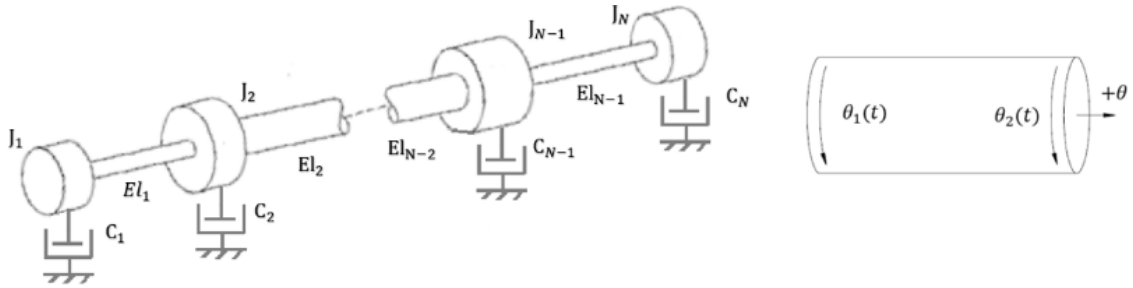


Figure 2. Single speed turbomachinery model (left) and shaft torsional element (right)

Assuming linear angle of twist along each element, inertia, stiffness and damping element matrices are defined as:

$$[J]_e = \frac{n^2 J}{6}\begin{bmatrix}2 & 1\\ 1 & 2\end{bmatrix};\ [K]_e = n^2 k_t\begin{bmatrix}1 & -1\\ -1 & 1\end{bmatrix};\ [C]_e = n^2 C\begin{bmatrix}1 & -1\\ -1 & 1\end{bmatrix}. \qquad (2-4)$$

where n is the speed of the element relative to the reference shaft and J, k_t and C are the polar mass moment of inertia, torsional stiffness and damping of each shaft element. Besides, the torques applied to the actual model shall be converted to the equivalent model and the angular displacement calculated using the equivalent model shall be converted back to the actual model. This can be accomplished with eq. 5-6, where the subscript "eq" denotes equivalent model and "a" actual model:

$$T_{eq} = nT_a;\ \ \theta_a = n\theta_{eq} \qquad (5-6)$$

3 Torsional vibration analysis overview

According to API [5], torsional analysis is based on the solution of eq. 1 in three different forms:

Undamped torsional analysis: since damping in almost all practical turbomachinery is very small, for practical purposes, undamped natural frequencies are no different from the damped ones. This analysis consists of solving eq. 1 ignoring the damping and with no torque applied (free vibration), which results in the Eigenvalue problem, where the eigenvalues are the TNFs squared and the eigenvectors are the mode shapes. Detailed solution procedure can be found in Inman [6]. TNFs can be plotted along with excitation sources on Campbell Diagrams to determine if there is any interference point within train operational range. For geared machines, Corbo [8] recommends using one diagram for each rotor or alternatively, to plot all information on a single diagram with all excitations referenced to the system equivalent speed, typically, the motor speed. The second method is applied in this work.

Steady-state torsional response analysis: if there is any interference point (resonance) in the operating region, then a steady-state torsional analysis is required. In this case, eq. 1 is solved for each resonance point, applying the excitation torque and damping and calculating the cyclic torques and stresses in all train components, that shall demonstrate infinite fatigue life. Corbo [2] and API [5] provide guidelines for fatigue assessment, which is not discussed here. According to Inman [6], if [C] can be written as a linear combination of [J] and [K], Modal Analysis procedure can be applied, which consists of using the principle of orthogonality of the modes to transform [J], [C] and [K] to diagonal matrices, decoupling the equations of motion in a new modal coordinate system, solving them as independent differential equations and converting back to the physical coordinate system. Corbo [8] states that, in practice, most torsional analyses are performed with an empirical modal damping ratio (% of critical damping) applied to all elements and this method can be applied. Relevant individual damping sources cannot be incorporated in the model in this approach. If [C] is not a linear combination of [J] and [K], then the equations of motion need to be solved simultaneously. In this work, this was accomplished by rewriting the N 2nd order ODEs of eq. 1 as 2N 1st order ODEs using the state variable modeling and applying Laplace Transform to convert the 2N ODEs to algebraic equations, that is, time to frequency domain, that can be more easily solved.

Transient torsional response analysis: for turbomachinery trains driven by induction motors, API [5] states that short circuit is the most relevant transient analysis and it is required when the associated excitations generate resonance with one of the train modes having relevant activity at the motor air-gap (usually the first mode). Transient simulation is run to determine torque vs time for each element in the model, the design being acceptable

if the maximum shear stresses in the elements are below the shear yield strengths since fatigue is not a concern (rare event of short duration). In this work, the state variable equations are numerically integrated in the time domain using an adaptative stepsize Runge-Kutta method based on Dormand-Prince. According to Aho [9], short circuit torques can reach 3-15 times motor rated full load torque and have the form of eq. 7:

$$T_{sc}(t) = -T_{rated}\left(T_1 e^{-\frac{t}{a1}}\sin(\omega_{feed}t) - T_2 e^{-\frac{t}{a2}}\sin(2\omega_{feed}t)\right) \tag{7}$$

where T_{rated} is the motor rated torque, ω_{feed} is the electrical feed frequency and T_1, T_2, a_1, a_2 are constants dependent on motor design. For 3-phase short circuits, $T_2 = 0$ while for 2-phase, typically, $T_2 = T_1/2$.

4 Computational code for torsional analysis of geared turbomachinery trains

The computational code for modeling and analyzing geared turbomachinery trains was developed in MATLAB. Code assumptions and input data required are:

Code assumptions: continuous system can be modeled using discrete elements; coupling between torsional and lateral vibration is not considered; gears are assumed rigid, without backlash or damping; for determination of TNFs and mode shapes, damping is negligible; for forced response calculations, forcing torques are harmonic; for forced steady-state response, the system is linear, a consequence of small angular deflections; if VFD is used, there is no feedback signal from mechanical system to VFD (no electro-mechanical interaction).

Input data: mass-elastic data (nodes and elements definition), speed ratio of each node and element, operating speed, driver type (fixed or variable speed), damping, excitation orders (1x, 2x, etc.), steady-state torque applied to each node (magnitude, phase and frequency); short circuit initial conditions (angular position and speed), eq. 7 parameters and *ode45* absolute and relative errors allowed per step (ode45 is a MATLAB ODE solver for equations in the form $y' = f(t, y)$ based on an adaptative stepsize Runge-Kutta method, the Dormand-Prince).

The code was validated by comparison with other works. One case of a multiple branched geared system from Wu [10] is presented here, the original train scheme and the equivalent single speed model are shown in fig. 3, detailed train data is omitted. Eigenvalue analysis was performed, five first non-zero TNFs were calculated, considering and neglecting shaft inertia. Damping was modeled as discrete dampers and Newmark Direct Integration Method was applied by Wu [10] to directly solve 2nd order ODEs. Forced response due to a torque applied at node 1 was calculated using 3 different values for the dampers. A comparison between the results obtained by Wu [10] and the code presented in this paper is provided in table 1. Results agreement is obvious.

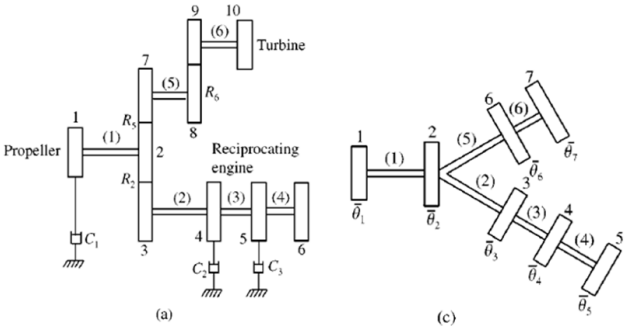


Figure 3. Single speed turbomachinery model (left) and shaft torsional element (right)

Table 1. Results comparison between Wu [10] and this work – undamped and steady-state analysis

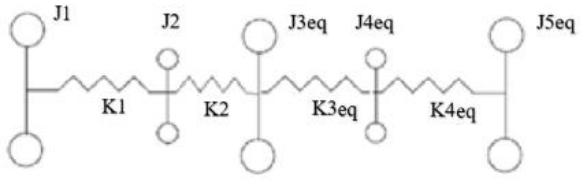
Mode	Natural Frequencies (rad/s)			
	Shaft mass neglected		Shaft mass considered	
	Wu [10]	Present code	Wu [10]	Present code
1	23.0899	23.0900	23.0870	23.0867
2	41.3228	41.3231	41.2902	41.2896
3	217.6013	217.6012	215.2224	215.2024
4	376.9155	376.9228	376.6524	376.6640
5	712.6985	712.6906	710.4786	710.8485

Steady-State Forced Response		
C	Maximum node 1 amplitude	
N.m.s/rad	Wu and Chen	Present code
x	0.077	0.0764
3x	0.052	0.0514
5x	0.037	0.0365

5 Case study – Electric Motor Driven Compressor

The application of the code to the torsional analysis of a geared turbomachinery train is demonstrated with a case adapted from Vance [4]. The train scheme is the same of fig. 1, with the following mass-elastic data: Motor: $J = 8$ kgm²; Motor output shaft: Ø80mm x 180 mm (AISI 4140). Gears: Low speed gear: $J = 0.7$ kgm²; High speed gear: $J = 0.06$ kgm². LS Coupling: $J = 0.25$ kgm², $k_t = 1.2*10^6$ Nm; HS Coupling: $J = 0.05$ kgm², $k_t = 3.4*10^6$ Nm. Compressor: $J = 0.8$ kgm²; Compressor input shaft: Ø60mm x 300 mm (AISI 4140).

The train is driven by a 2-pole induction motor at 50 Hz line frequency, 1550 kW, gear ratio (n) = 2.0 (teeth number: 30 and 15 for gear and pinion). Equivalent single speed model referred to motor speed is shown in fig. 4:



Legend

Inertias		Stiffnesses	
J1	Motor	K1	Motor output shaft
J2	Half LS coupling	K2	LS Coupling
J3eq	Gears + half couplings	K3eq	HS Coupling
J4eq	Half HS coupling	K4eq	Compressor input shaft
J5eq	Compressor		

Figure 4. Simplified single speed torsional model schematic

The undamped torsional analysis was performed and natural frequencies calculated: 0 Hz (rigid body mode), TNF1=69.5 Hz, TNF2=223.3 Hz, TNF3=786.6 Hz and TNF4=2024.4 Hz.

Two cases were considered: case 1, fixed speed motor and case 2, VFD motor with speed variation from 70-110% of the nominal speed (10% separation margin required by API [5] included). The following excitation orders are plotted in the Campbell Diagrams: Case 1 (fig. 5): mechanical sources (unbalance, misalignment, blade passing frequency, gear meshing frequency): 1x, 2x, 4x, 12x, 30x of the motor speed; electrical: 1x and 2x of electrical line frequency. Case 2 (fig. 6): mechanical sources: 1x, 2x, 4x, 12x, 30x motor speed; VFD harmonics: 1x, 2x, 6x, 12x, 18x, 24x electrical frequency supplied to motor by the VFD, which is equal to motor speed for a 2-pole motor.

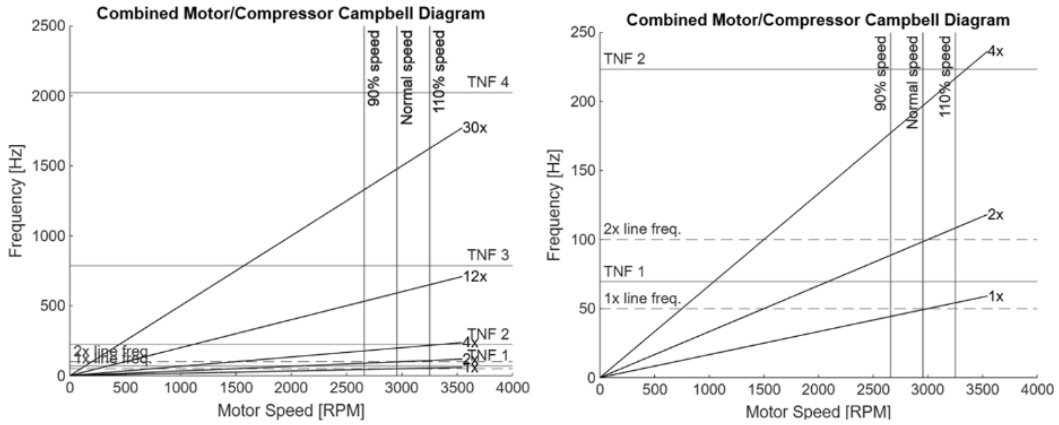


Figure 5. Campbell Diagram, complete (left) and zoomed view (right) – fixed speed motor

In fig. 5, TNFs are represented as continuous horizontal lines, operation speed range (separation margin included) by vertical lines, mechanical excitations by inclined lines and electrical excitation by dashed horizontal lines. Since there was no interference in the operation range, steady-state forced response analysis was not required.

For the VFD motor (fig. 6), the wider operation range combined with extra VFD harmonics caused interference points identified as I1, I2 and I3. Besides, an extra interference point I4 with TNF1 at maximum continuous speed was considered to account for possible inter-harmonic excitation, as recommended by API [5]. Steady-state response analysis shall be performed for each interference point, here only the results for point I2 and I4 are presented in table 2. For point I2, the TNF2 can be excited by the 6x VFD harmonic when the motor is operating at 2233 rpm (1/6*TNF2). During the design phase, VFD torque harmonics shall be provided by the VFD

manufacturer, here a conservative value of 10% motor rated torque recommended by Corbo [8] was used. For point I4, it was assumed an 1% motor rated torque exciting the TNF1 with the motor operating at max speed (3250 rpm), as recommended by API [5]. Conservative modal damping ratio of 1% for all modes was applied.

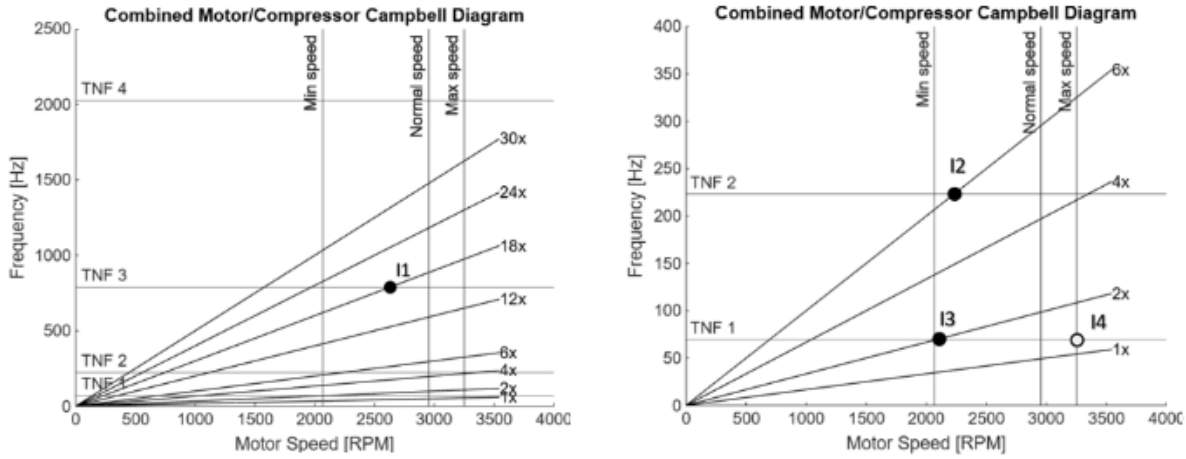


Figure 6. Campbell Diagram, complete (left) and zoomed view (right) – VFD motor

Table 2. Calculated twisting angles, torques and nominal cyclic shear stresses for the train elements

Element		Interference 2			Interference 4		
Id	Name	Twisting angle (°)	Transmitted Torque (Nm)	Cyclic shear stress (MPa)	Twisting angle (°)	Transmitted Torque (Nm)	Cyclic Shear stress (MPa)
1	Motor shaft	0,0112	349,5	3,5	0,0277	862,9	8,6
2	LS Coupling	0,0147	307,2	NA	0,0413	864,8	NA
3	HS Coupling	-0,0057	-338,3	NA	-0,0061	-361,4	NA
4	Compressor shaft	-0,0571	-375,6	-8,9	-0,0539	-354,8	-8,4

For each interference point, the forced response was determined, i.e. magnitude and phase of each node angular displacement. With this result, each element twisting angle, transmitted torque and cyclic shear stress were calculated (table 2). Even though excitation torque for I4 was only 1/10 of the torque applied for point I2 analysis, shear stresses were much higher for the motor shaft and of similar magnitude for the compressor shaft since the 1st mode was excited. Shear stresses were not calculated for the couplings because they have complex geometry (flexible elements, bolted connections, spacers, etc.), which requires coupling manufacturer advice to define maximum cyclic torque allowed. With torques and cyclic stresses calculated, fatigue analysis, which is not presented here, shall be performed for all elements, safety factor shall be higher than 2.0, as per API [5].

Short circuit torque has 1x and 2x electrical feed frequency components (eq. 7). For the fixed speed motor, these frequencies are constant and were represented by dashed lines in fig. 5, far from TNF1. However, when VFD motor is used, these excitations become speed-dependent and appear as sloped lines, the 2x component causes resonance with the TNF1 (point I3) when the motor is at 2085 rpm (1/2*TNF1), as shown in fig. 6. Short circuit in this condition might be severe and API [5] requires a short circuit response analysis. The following parameters were adopted in eq. 7: T_{rated}=5.0 kNm, T_1=6.0, $T_2 = 3.0$ (for 3-phases short circuit, $T_2 = 0$), a_1=0.030, a_2=0.026 and ω_{feed}=218.3 rad/s (1/2*TNF1). Initial angular speed of each node was the operational speed (2085 rpm) and initial angular positions were defined based on the mean torque transmitted at the operational speed. The state variable equations of motion were numerically integrated using ode45. Angular displacement response as function of time for each node was calculated and actual twisting angle of each element obtained (corrected by gear ratio), along with respective transmitted torques and shear stresses. 3-phase and 2-phase short circuit excitation and response torques generated at the motor shaft are presented in fig. 7, normalized by the motor rated torque (per unit, p.u.).

As shown in fig. 7, the maximum 3-phase short circuit response torque achieved 2.96 p.u. (abs) and decreased to less than 1.0 p.u (abs) in few cycles, while 2-phase short circuit achieved 5.46 p.u. (abs) and took multiple cycles

to achieve 1.0 p.u (abs), due to the resonance condition. With the calculated torque, maximum shear stresses and safety factor against shear yield can be calculated for the motor shaft. API [5] acceptance criteria is simply survival (maximum shear stresses lower than shear yield strength), there is no minimum safety factor recommended.

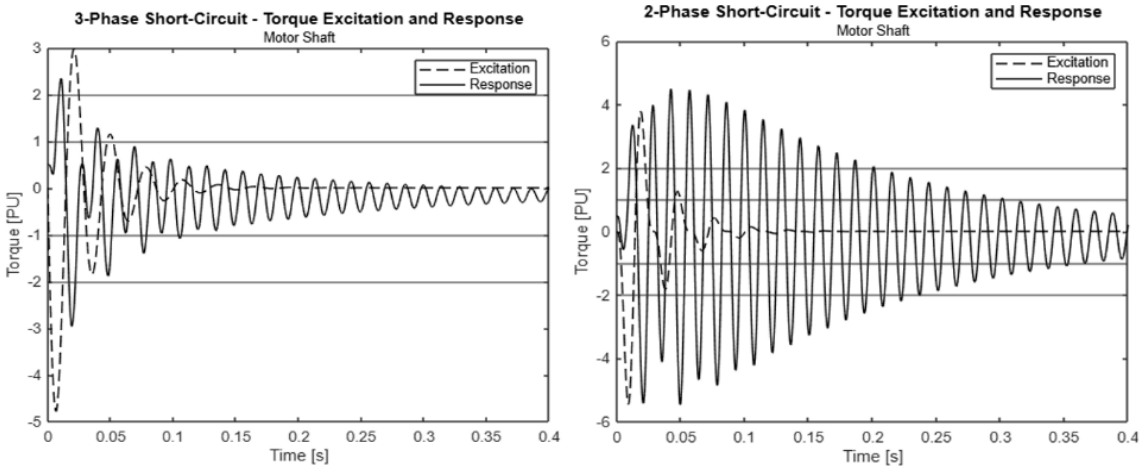


Figure 7. 3-phase (left) and 2-phase (right) short circuit excitation and response torques at motor shaft

6 Conclusions

The basis of torsional integrity assessment of geared turbomachinery train was presented, following API guidelines for modeling and analysis. The FEM computational code developed can be applied to the torsional analysis of single or multi-branched systems to obtain the equations of motion and perform all the calculations required by API: natural frequencies, mode shapes, Campbell Diagrams, steady-state and transient forced responses. The case study demonstrated that VFD driven trains require careful torsional vibration analysis due to the wider operation range, harmonics and inter-harmonics excitations caused by the VFD and the increased likelihood of a short circuit triggering a resonance with first mode due to the variation of the electrical frequency fed to the motor.

Acknowledgements. The authors are thankful for the financial support from CAPES.

Authorship statement. The authors hereby confirm that they are the sole liable persons responsible for the authorship of this work, and that all material that has been herein included as part of the present paper is either the property (and authorship) of the authors or has the permission of the owners to be included here.

References

[1] IOGP, *Report 653: Recommended Practices for electrification of oil and gas facilities*, 2022.
[2] Corcoran, J. P., Kocur, J. A., Mitsingas, M. C, ”Preventing undetected train torsional oscillations”, *Proceedings of the Thirty-Ninth Turbomachinery Symposium*, pp. 135-146, 2010.
[3] Kita, M., “Considerations in the Design of VFD Motor-Driven Compressors”. Asia Turbomachinery & Pump Symposia. Turbomachinery Laboratories, 2016.
[4] Vance, J. M., Zeidan, F. Y., & Murphy, B. G. *Machinery vibration and rotordynamics*. John Wiley & Sons, 2010.
[5] API, “API TR 684-1, API Standard Paragraphs - Rotordynamic Tutorial: Lateral Critical Speeds, Unbalance Response, Stability, Train Torsionals and Rotor Balancing”, First Edition, 2019.
[6] Inman, J. D., *Engineering Vibration*, 4th edition, Pearson, 2014.
[7] Walker, Duncan N., *Torsional Vibration of Turbomachinery*. 1st ed., McGraw-Hill. 2004.
[8] Corbo, M. A, Malanoski, S. B., “Practical Design Against Torsional Vibration”, *Proceedings of the Twenty-Fifth Turbomachinery Symposium,* pp. 189-222. 1996.
[9] Aho, T., Nerg, J., Baum, C. “Torsional excitation upon short-circuit in induction motors in conventional and high-speed trains”. *Proceedings of the 46th Turbomachinery Symposium*. Texas A&M Turbomachinery Laboratories, 2017
[10] Wu, J. S., and Chen, C. H., "Torsional vibration analysis of gear-branched systems by finite element method.", Journal of sound and vibration 240(1), pp. 159-182, 2001.